

# Photochemistry of Hydrogen Iodide–Acetylene Complexes in Solid Krypton

Samuel A. Abrash<sup>†</sup> and George C. Pimentel<sup>\*‡</sup>

Laboratory of Chemical Biodynamics, Lawrence Berkeley Laboratory, University of California, Berkeley, California 94720 (Received: January 27, 1989)

Hydrogen iodide–acetylene complexes in a krypton matrix at 12 K have been photolyzed with a medium-pressure mercury lamp. Infrared spectra identify products vinyl iodide and iodoacetylene. When HI·C<sub>2</sub>D<sub>2</sub> complexes are photolyzed, isotopic exchange occurs to produce DI·HCCD. Growth curves show that all three are primary products. As well, the growth curves show secondary photolysis of vinyl iodide and DI·HCCD, but apparently production and secondary photolysis of vinyl iodide only catalyze isotopic exchange. The growth curves obtained for HCCI and DCCI from HI·C<sub>2</sub>D<sub>2</sub> differ from those obtained from DI·C<sub>2</sub>H<sub>2</sub>. Short photolysis of HI·C<sub>2</sub>D<sub>2</sub> gives almost exclusively HD·DCCI whereas short photolysis of DI·C<sub>2</sub>H<sub>2</sub> gives HD·HCCI. Thus, the hydrogen atom in the hydrogen iodide always ends up in the molecular hydrogen product. We conclude that photolytic production of iodoacetylene involves hydrogen atom abstraction from acetylene by the energetic hydrogen iodide.

## Introduction

The matrix photolysis of hydrogen halide–acetylene complexes is of special interest because the complex is considered to have a well-defined and known T-shaped geometry.<sup>1–3</sup> Thus held in proximity and in fixed orientation, the complex offers a favorable opportunity to address the question of how this geometry affects the photochemistry and how the upper electronic state is related to the excited states of the component molecules. Our first approach to these issues is to determine the photochemical products for the hydrogen iodide–acetylene complex. In a subsequent paper,<sup>4</sup> we will investigate product branching as a function of photolysis wavelength.

## Experimental Section

The cryostat was an Air Products Model CS202 closed-cycle helium refrigerator capable of cooling our substrate, either cesium iodide or sodium chloride (Harshaw), to 12 K. The cryostat was equipped with a hydrogen gauge and an Au (0.07% Fe) vs Chromel thermocouple for temperature determinations as well as a resistance heater for annealing or high-temperature depositions. Matrix temperatures were measured to  $\pm 0.5$  K by using the thermocouple and the hydrogen pressure gauge. The cryostat was placed in the beam path of an FTIR spectrometer for sample analysis following depositions, photolyses, and warm-ups. It was fitted with CsI windows in the IR ports and a quartz window in the photolysis port.

The FTIR was an IBM Model IR97 operated over the spectral range 400–4000 cm<sup>-1</sup> at 0.25 or 0.5-cm<sup>-1</sup> resolution and with wavelength accuracy of 0.1 cm<sup>-1</sup>.

To prepare mixtures, the desired amount of HI was introduced into the vacuum line. The empty mixture bulb was then opened and the hydrogen iodide frozen in liquid nitrogen. The bulb was then reclosed and the procedure repeated, first, for acetylene and then for krypton (which has a vapor pressure of 2.20 Torr at 77 K). After the Kr was added, the mixture bulb was closed, and the mixture was thawed and then allowed to mix diffusively for at least 6 h.

Hydrogen iodide (Matheson, 98%), acetylene (Pacific Oxygen Co., 99.6%), and acetylene-*d*<sub>2</sub> (MSD Isotopes, 99% D) were purified by bulb-to-bulb distillation to remove noncondensable gases and halogens. The purified gases were stored in glass bulbs fitted with a Teflon stopcock and Viton O-ring. The HI was stored in a blackened bulb. DI (MSD Isotopes) was used, without further purification. For experiments in which DI was used, all vacuum lines were repeatedly passivated with D<sub>2</sub>O. The final passivation was with pure DI. In some experiments, passivation was done

TABLE I: Product Frequencies and Intensities after 402-min Mercury Lamp Photolysis of HI/C<sub>2</sub>H<sub>2</sub>/Kr = 1/1/100

freq, cm <sup>-1</sup>	rel peak abs	assign
3314.6	22	C <sub>4</sub> HI
3305.8	(100)	$\nu_1$ (C <sub>2</sub> HI)
2053.5	10	$\nu_2$ (C <sub>2</sub> HI)
1975.0	22	?
1587.2	28	CH <sub>2</sub> CHI
1586.5	19	CH <sub>2</sub> CHI
1585.6	13	CH <sub>2</sub> CHI
1436.5	32	?
1368.6	9	CH <sub>2</sub> CHI
1237.3	21	CH <sub>2</sub> CHI
1234.9	11	C <sub>4</sub> HI
952.1	22	CH <sub>2</sub> CHI
625.7	32	C <sub>4</sub> HI
624.1	37	$\nu_4$ (C <sub>2</sub> HI)
623.8	37	$\nu_4$ (C <sub>2</sub> HI)

only with DI. Typical D<sub>2</sub>O passivations resulted in sample deuteration of between 67 and 85%. Typical DI passivations lead to enrichments of 67% to 90%. Kr (99.995%) was used without further purification.

All matrices were deposited at 20.0  $\pm$  0.4 K. deposition rates varied from 0.5 to 2.0 mmol/h, with the amounts deposited varying from 1 to 4 mmol.

The photolysis source for these experiments was a medium-pressure mercury lamp (General Electric AH-4, 100 W) with its Pyrex housing cut off and the output focused by either a 1.5-in. diameter, 5-cm focal length fused silica lens (Oriel) or a 1.0-in. diameter, 7.5-cm focal length fused silica lens (Optics for Research).

The photolysis procedure was as follows. With the cryostat rotated so that the radiation shield blocked the photolysis beam, the lamp was turned on and allowed to warm for a minimum of 10 min. Thereafter, the cryostat was rotated to place the matrix sample in the beam path. All photolyses took place on the front face of the CsI substrate; i.e., the light did not pass through the substrate before reaching the sample. After each photolysis a new IR spectrum was recorded in order to obtain kinetic information. After sufficient kinetic information was obtained, the sample was annealed by warming, usually at the rate of 0.5 K min<sup>-1</sup>, to a temperature between 45 and 50 K followed by cooling at an

(1) Legon, A. C.; Aldrich, P. D.; Flygare, W. H. *J. Chem. Phys.* **1981**, *75*, 625.

(2) McDonald, S. A.; Johnson, G. L.; Keelon, B. W.; Andrews, L. W. *J. Am. Chem. Soc.* **1980**, *102*, 2892.

(3) Andrews, L.; Johnson, G. L.; Kelsall, B. J. *J. Phys. Chem.* **1982**, *86*, 3374.

(4) Abrash, S. A.; Pimentel, G. C. *J. Phys. Chem.*, following paper in this issue.

<sup>†</sup> Present address: Department of Chemistry, University of Pennsylvania, Philadelphia, PA 19123.

<sup>‡</sup> Deceased June 18, 1989.

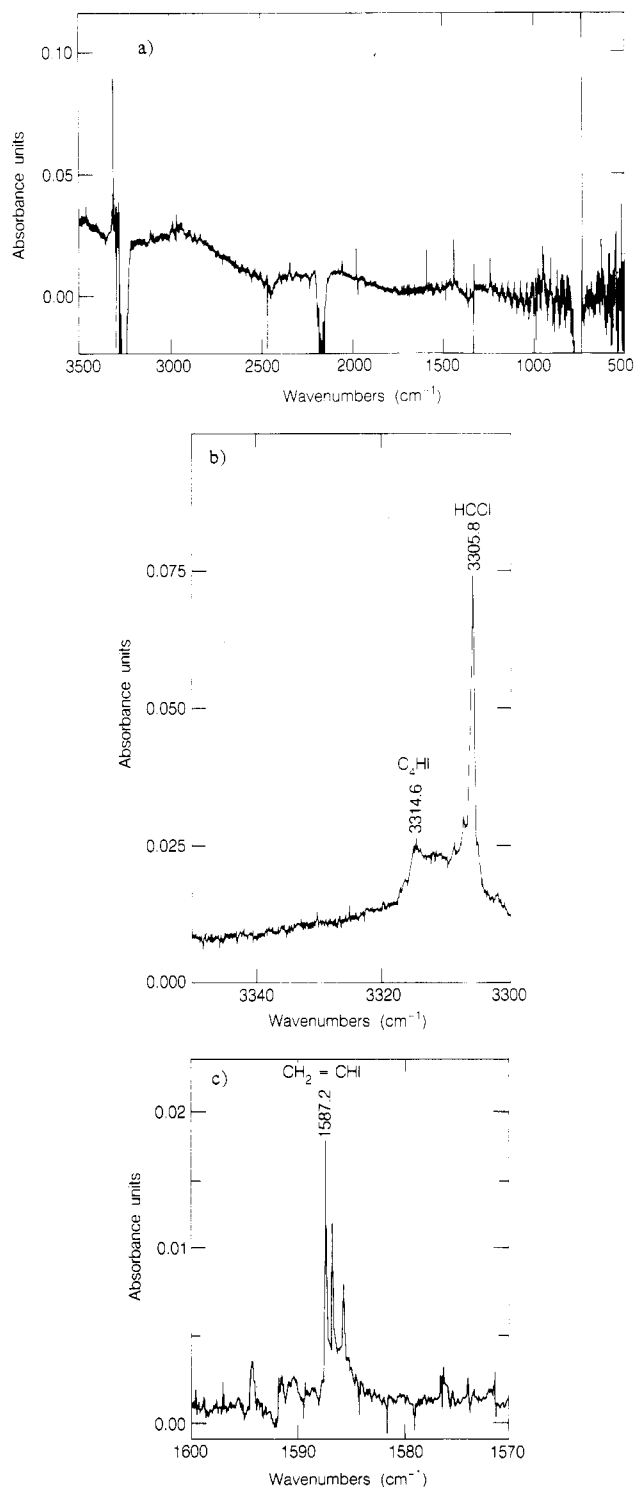


**Figure 1.** Products after 402-min Hg lamp photolysis, HI/C<sub>2</sub>H<sub>2</sub>/Kr = 1/1/100: (a) 500–3500 cm<sup>-1</sup>; (b) C–H stretching region, 3300–3350 cm<sup>-1</sup>; (c) C=C stretching region, 1570–1600 cm<sup>-1</sup>.

approximate rate of 1 K min<sup>-1</sup>. When the substrate temperature returned to 12 K, an IR spectrum was recorded.

## Results

HI/C<sub>2</sub>H<sub>2</sub>/Kr = 1/1/100. After photolysis, difference spectra revealed growth of a number of products. Table I lists the product frequencies and peak intensities after 402 min of photolysis. Figure 1a shows a survey difference spectrum over the range 500–3500 cm<sup>-1</sup>, while Figure 1b and Figure 1c show key spectral ranges, 3300–3350 and 1570–1600 cm<sup>-1</sup>, respectively. Examination of product intensity vs photolysis time indicated two distinctive growth behaviors, as displayed in Figure 2. The product feature at 1587.2 cm<sup>-1</sup> grows rapidly and then decreases, apparently due to sec-

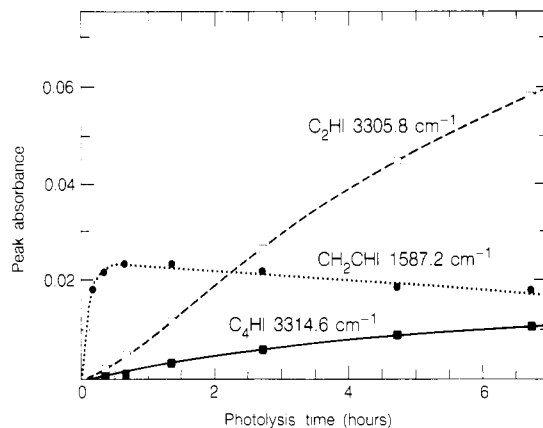


**Figure 2.** Product growth during photolysis, HI/C<sub>2</sub>H<sub>2</sub>/Kr = 1/1/100.

**TABLE II: Product Frequencies and Intensities after 480-min Mercury Lamp Photolysis of HI/C<sub>2</sub>D<sub>2</sub>/Kr = 1/1/100**

freq, cm <sup>-1</sup>	rel peak abs	assignt
3334.0	29	$\nu_1$ (C <sub>2</sub> HD)
3328.5	39	$\nu_1$ (DI-C <sub>2</sub> HD)
3326.0	19	$\nu_1$ (DI-C <sub>2</sub> HD)
3306.1	54	$\nu_1$ (C <sub>2</sub> HI)
2584.0	(100)	$\nu_1$ (C <sub>2</sub> DI)
2582.1	24	$\nu_1$ (C <sub>2</sub> HD)
2577.7	42	$\nu_3$ (DI-C <sub>2</sub> HD)
2053.8	6	$\nu_2$ (C <sub>2</sub> HI)
1975.2	4	$\nu_2$ (C <sub>2</sub> DI)
1563.2	6	$\nu_{DI}$ (DI-C <sub>2</sub> HD)
1562.5	8	$\nu_{DI}$ (DI-C <sub>2</sub> HD)
684.2	35	$\nu_5$ (DI-C <sub>2</sub> HD)
683.0	31	$\nu_5$ (DI-C <sub>2</sub> HD)
679.4	190	$\nu_5$ (C <sub>2</sub> HD)
626.1	22	$\nu_4$ (C <sub>2</sub> HI)
623.9	27	$\nu_4$ (C <sub>2</sub> HI)
516.4	56	$\nu_4$ (C <sub>2</sub> HD)
488.9	25	$\nu_4$ (C <sub>2</sub> DI)
488.0	31	$\nu_4$ (C <sub>2</sub> DI)

ondary photolysis. In contrast, the prominent absorption at 3305.8 cm<sup>-1</sup> has a sigmoidal growth contour but with nonzero slope at short times. Other bands that grew in concert with 3305.8 cm<sup>-1</sup> were 2053.5, 625.7, 624.1, and 623.8 cm<sup>-1</sup>. Features that grew in concert with 1587.2 cm<sup>-1</sup> are the product bands at 1586.5, 1368.6, 1237.3, and 952.1 cm<sup>-1</sup>.

Comparison of these product frequencies to gas-phase spectra readily identifies two products. The infrared spectrum of gaseous iodoacetylene,<sup>5,6</sup> HCCI, shows bands at 3326, 2060, 630, and 488 cm<sup>-1</sup>. The first three correspond closely to bands with the growth behavior of 3305.8 cm<sup>-1</sup> while 488 cm<sup>-1</sup> is in a spectral region of high noise level. Plainly, HCCI is a product with some of its growth due to secondary photolysis.

In a similar way vinyl iodide is identified as the second major product by the gas-phase absorptions of CH<sub>2</sub>CHI, 1593, 1376, 1229, and 948 cm<sup>-1</sup>. Its growth behavior indicates it quickly reaches a maximum intensity and then decreases due to secondary photolysis.

Among the remaining features, 3314.6 cm<sup>-1</sup> had the growth behavior shown in Figure 2 and it grew in concert with 1234.9 and the features near 625 cm<sup>-1</sup>. These are assigned to iodoacetylene, HC<sub>4</sub>I, by analogy to the similar absorptions found by Klaboe et al.<sup>7</sup> for bromodiacyetylene: 3335, 1234.5, and 623 cm<sup>-1</sup>.

HI/C<sub>2</sub>D<sub>2</sub>/Kr = 1/1/100. Figure 3a shows the difference spectrum obtained after 480 min of photolysis of an HI/C<sub>2</sub>D<sub>2</sub> mixture. Figure 3b and Figure 3c show the regions 3300–3350

(5) Carpenter, J. H.; Rimmer, D. F.; Whiffen, D. H. *J. Chem. Soc., Faraday Trans. 2* **1972**, *68*, 1914.

(6) Rogstad, A.; Cyvin, S. J. *J. Mol. Struct.* **1974**, *20*, 373.

(7) Klaboe, P.; Kloster-Jensen, E.; Cyvin, S. L. *Spectrochim. Acta* **1987**, *23A*, 2733.

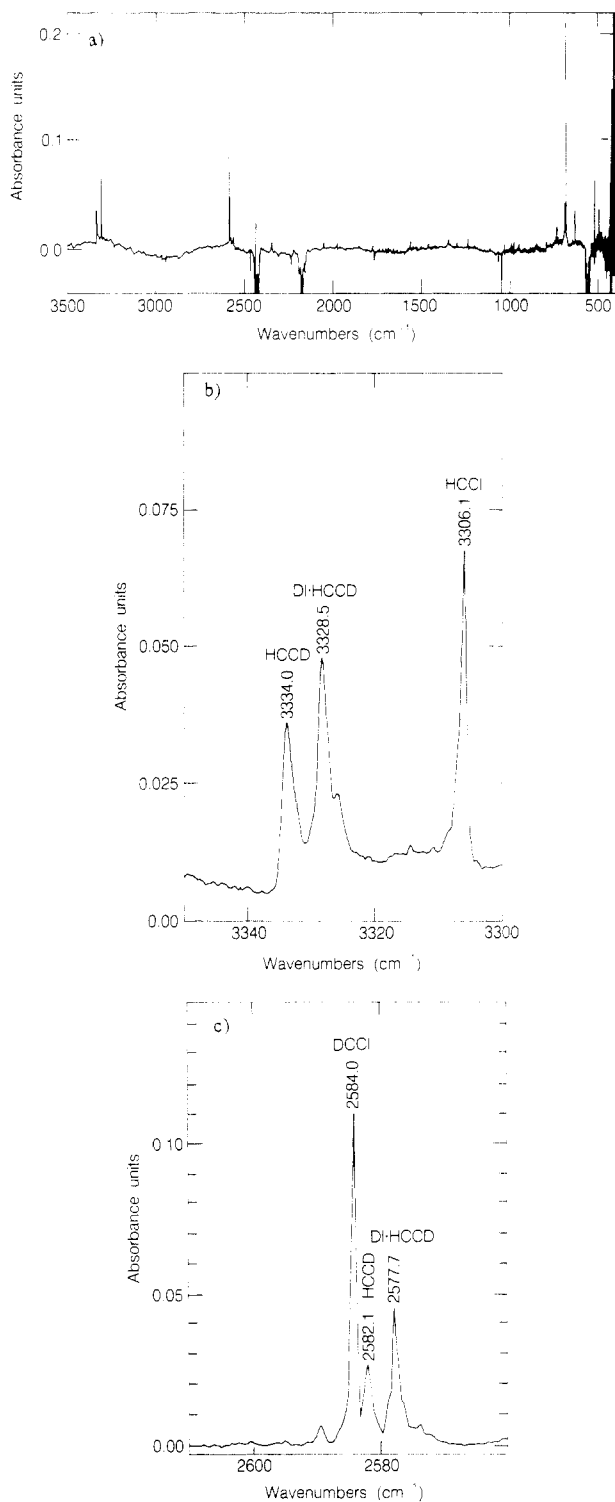


**Figure 3.** Products after 480-min Hg lamp photolysis,  $\text{HI}/\text{C}_2\text{D}_2/\text{Kr} = 1/1/100$ : (a) 450–3500  $\text{cm}^{-1}$ ; (b) C–H stretching region, 3300–3350  $\text{cm}^{-1}$ ; (c) C–D stretching region, 2560–2620  $\text{cm}^{-1}$ .

and 2560–2620  $\text{cm}^{-1}$ , respectively. Table II, which lists the product frequencies, includes the absorptions assigned to HCCI but not those assigned to  $\text{CH}_2\text{CHI}$ , both as expected. The second most intense feature, at 2584.0  $\text{cm}^{-1}$ , can be assigned as the C–D stretching motion of DCCI, giving an isotope shift of 1.28. The  $\nu_2$  mode of DCCI is seen at 1975.2  $\text{cm}^{-1}$ , sharing the deuterium isotope shift. Thus, the HCCI  $\nu_1$  and  $\nu_2$  vibrations show an overall deuterium shift of  $(1.28)(1.04) = 1.33$ , corroborating the identification. Again, isotope shift (1.28) readily identifies 488.9 and 488.0  $\text{cm}^{-1}$  as  $\nu_4$  of DCCI.

There remain quite a number of unassigned features (including the most intense product band, 679.4  $\text{cm}^{-1}$ ) that reveal a product

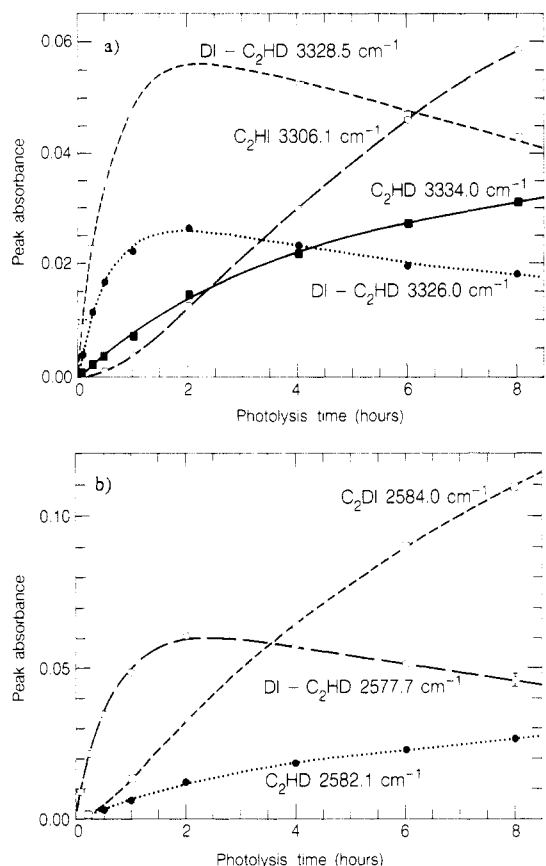


**Figure 4.** Product growth during photolysis,  $\text{HI}/\text{C}_2\text{D}_2/\text{Kr} = 1/1/100$ : (a) C–H stretching region; (b) C–D stretching region.

not detected in the  $\text{HI}-\text{C}_2\text{H}_2$  experiments. The 679.4- $\text{cm}^{-1}$  feature is immediately recognized as HCCD with other appropriately placed absorptions at 3328.5, 2577.7, and 516.4  $\text{cm}^{-1}$ . These frequencies match nicely the absorptions of gaseous HCCD, 677.8, 3335.6, and 518.4  $\text{cm}^{-1}$ ,<sup>8</sup> and of HCCD in  $\text{N}_2$  matrix, 694.5/689.5, 3332.5, and 2580  $\text{cm}^{-1}$ .<sup>9</sup> The growth behaviors of typical bands are shown in Figure 4. As in Figure 2, the HCCI and DCCI show sigmoidal growth whereas the HCCD absorptions grow in as primary photolysis products, and then they are diminished by secondary photolysis.

The absence, in Table II, of absorptions clearly assignable to vinyl iodide is not surprising. None of the  $\text{CH}_2\text{CHI}$  features listed in Table I was particularly intense, and for monodeuteriovinyl iodide, there are three distinct structures to share this intensity.

One final datum of interest in this experiment is the relative intensity of the HCCI and DCCI features. If the isotopes were distributed in proportion to the H/D ratio, HCCI should be half as probable as DCCI. Because of the factor of 2 lower absorption coefficient of the C–D vibrations, the ratio of the C–D stretching mode intensity (at 2584.0  $\text{cm}^{-1}$ ) to that of the C–H stretching mode (at 3306.1  $\text{cm}^{-1}$ ) is expected on this basis to be near unity. The measured ratio after 480 min of photolysis is  $100/54 = 1.85$ . This translates into an almost two-to-one preference for elimination of HD over elimination of  $\text{D}_2$ . More important, the C–D/C–H intensity ratio changes rapidly with time, as shown in Figure 5. At a photolysis time of 30 min, the preference for DCCI over HCCI is near 10. Plainly there is a very strong preference for the HI hydrogen to end up as HD.

At long times, this ratio seems to be approaching an asymptotic value of 3.6 as the H and D positions become scrambled.

$\text{DI}/\text{HI}/\text{C}_2\text{H}_2/\text{Kr} = 0.69/0.31/1.0/100$ . As before, spectra are displayed for key regions in Figure 6, and product frequencies

(8) Shimanouchi, T. Report NSRDS—NBS 39; National Bureau of Standards, U.S.: Gaithersburg, MD, June 1972.

(9) Bagnanskis, N. I.; Bulanin, M. O. *Opt. Spectrosc.* **1972**, *31*, 525.

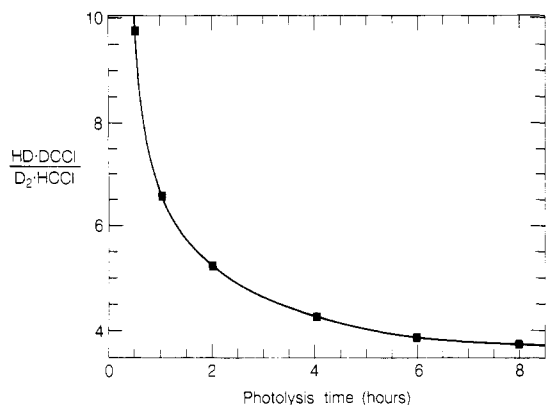


Figure 5. Relative yield of C<sub>2</sub>DI/C<sub>2</sub>HI, HI/C<sub>2</sub>D<sub>2</sub>/Kr = 1/1/100.

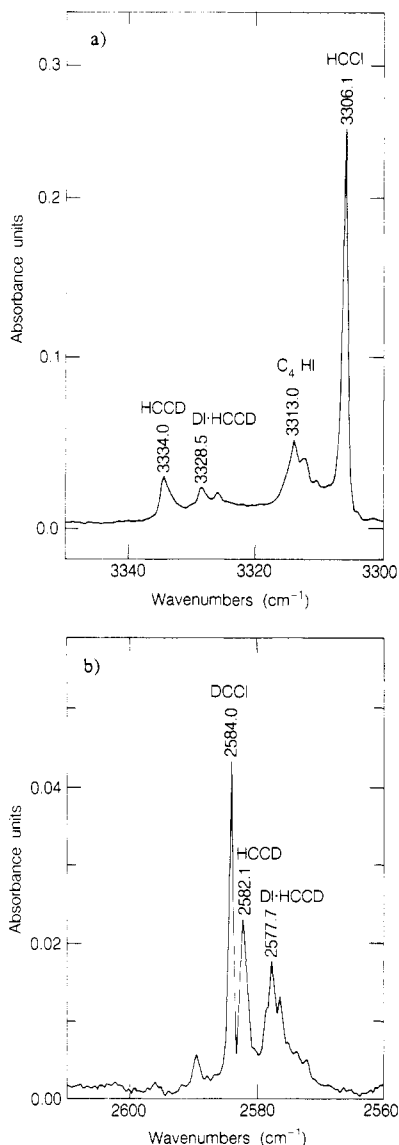


Figure 6. Product growth rate after 480-min Hg lamp photolysis, DI/HI/C<sub>2</sub>H<sub>2</sub>/Kr = 0.69/0.31/1/100: (a) C-H stretching region, 3300–3350 cm<sup>-1</sup>; (b) C-D stretching region, 2560–2620 cm<sup>-1</sup>.

are listed in Table III. The growth curves, shown in Figure 7, show a rapid growth of HCCD (e.g., see 3328.1 cm<sup>-1</sup>) much like that seen in Figure 4a. In contrast, the absorption at 3306.1 cm<sup>-1</sup> due to HCCI does not display the clear sigmoidal growth that is seen in Figure 4a, whereas the DCCI feature at 2584.0 cm<sup>-1</sup> does show sigmoidal growth (see Figure 7b).

Once again, the relative amounts of HCCI and DCCI vary with photolysis time, as shown in Figure 8. For this experiment, the

TABLE III: Product Frequencies and Intensities after 480-min Mercury Lamp Photolysis of DI/HI/C<sub>2</sub>H<sub>2</sub>/Kr = 0.69/0.31/1/100

freq, cm <sup>-1</sup>	rel peak abs	assignt
3334.5	12	$\nu_1$ (C <sub>2</sub> HD)
3328.7	8	$\nu_1$ (HI-C <sub>2</sub> HD)
3314.2	21	$\nu_1$ (C <sub>4</sub> HI)
3306.1	(100)	$\nu_1$ (C <sub>2</sub> HI)
2584.0	18	$\nu_1$ (C <sub>2</sub> DI)
2582.3	9	$\nu_3$ (C <sub>2</sub> HD)
2053.8	9	$\nu_2$ (C <sub>2</sub> HI)
1235.1	14	2 $\nu_4$ (C <sub>2</sub> HI)
679.6	50	$\nu_5$ (C <sub>2</sub> HD)
625.9	48	$\nu_4$ (C <sub>2</sub> HI)
623.9	59	$\nu_4$ (C <sub>2</sub> HI)
516.4	16	$\nu_4$ (C <sub>2</sub> HD)

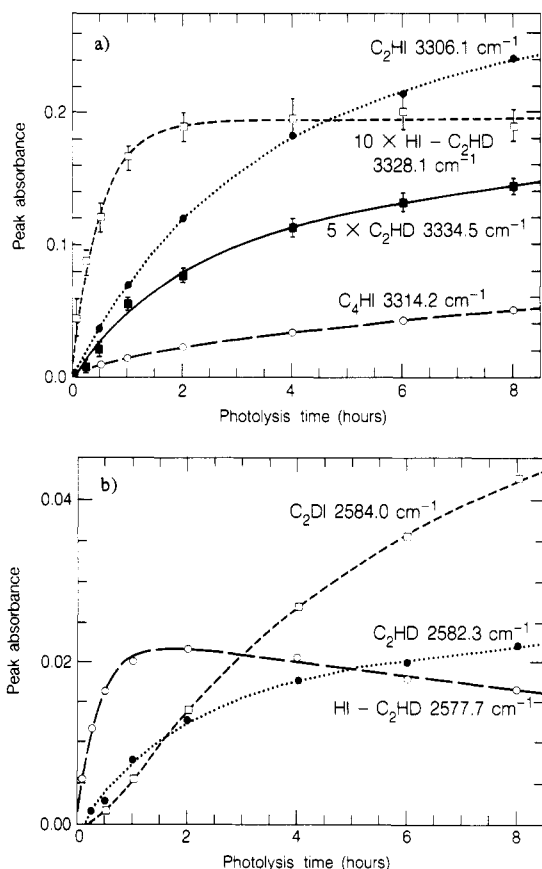


Figure 7. Product growth during photolysis, DI/HI/C<sub>2</sub>H<sub>2</sub>/Kr = 0.69/0.31/1/100: (a) C-H stretching region; (b) C-D stretching region.

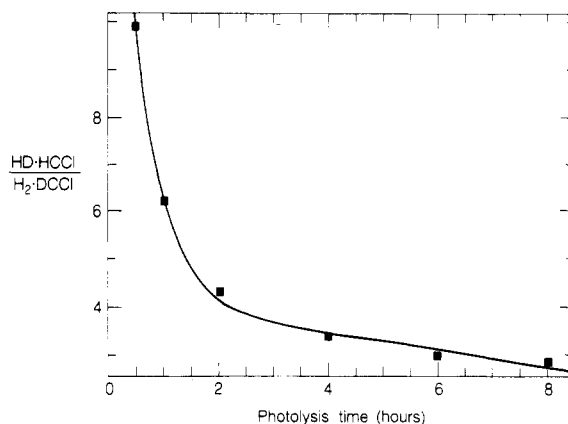
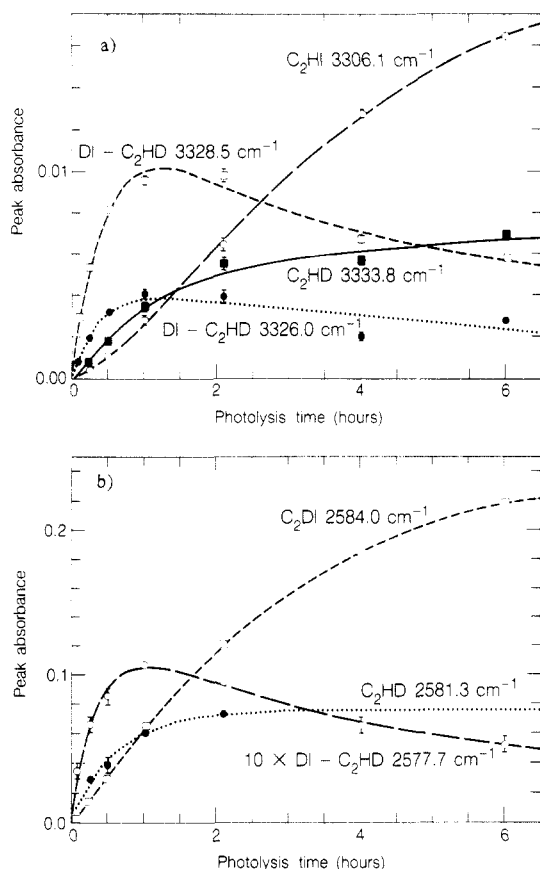


Figure 8. Relative yield of C<sub>2</sub>HI/C<sub>2</sub>DI, DI/HI/C<sub>2</sub>H<sub>2</sub>/Kr = 0.69/0.31/1/100.

H/D ratio would suggest an overall intensity ratio HCCI/DCCI = 3.35 whereas Figure 8 shows this ratio to be near 10 at 30 min. Once again, there is a strong preference for the DI deuterium to

**TABLE IV: Product Frequencies and Intensities after 360-min Mercury Lamp Photolysis of DI/HI/C<sub>2</sub>D<sub>2</sub>/Kr = 0.66/0.34/1/100**

freq, cm <sup>-1</sup>	rel peak abs	assignt
3333.8	3	$\nu_1(\text{C}_2\text{HD})$
3328.5	3	$\nu_1(\text{DI}\cdot\text{C}_2\text{HD})$
3306.1	8	$\nu_1(\text{C}_2\text{HI})$
2584.0	(100)	$\nu_1(\text{C}_2\text{DI})$
2577.7	2	$\nu_3(\text{DI}\cdot\text{C}_2\text{HD})$
969.9	7	$2\nu_4(\text{C}_2\text{DI})$
682.9	3	$\nu_5(\text{DI}\cdot\text{C}_2\text{HD})$
680.8	13	$\nu_5(\text{C}_2\text{HD})$
624.2	5	$\nu_4(\text{C}_2\text{HI})$
516.4	5	$\nu_4(\text{C}_2\text{HD})$
489.4	18	$\nu_4(\text{C}_2\text{DI})$
488.2	30	$\nu_4(\text{C}_2\text{DI})$

**Figure 9.** Product growth during photolysis, DI/HI/C<sub>2</sub>D<sub>2</sub>/Kr = 0.66/0.34/1/100: (a) C-H stretching region; (b) C-D stretching region.

end up as HD. At long times, the ratio seems to be approaching an asymptotic value of 2.8.

DI/HI/C<sub>2</sub>D<sub>2</sub>/Kr = 0.66/0.34/1.0/100. Product frequencies for this experiment are listed in Table IV, and key growth curves are shown in Figure 9. This time, 3306.1 cm<sup>-1</sup> due to HCCI shows clear sigmoidal character while 2584.0 cm<sup>-1</sup> of DCCI does not.

## Discussion

**Matrix Concentrations.** With the known bond lengths and conventional van der Waals radii, it is clear that C<sub>2</sub>H<sub>2</sub> will require two adjacent sites in the krypton lattice, implying 18 nearest neighbors. The HI molecule may be a bit large to fit in a single site, but we shall assume that it does. The T-shaped HI·C<sub>2</sub>H<sub>2</sub> complex will fit comfortably in a three-site vacancy, which will give it 32 nearest neighbors. With these assumptions and a statistical picture of matrix composition, we can calculate the populations of complexes.

At matrix ratios HI/C<sub>2</sub>H<sub>2</sub>/Kr = 1/1/100, the statistical fraction of isolated HI will be 70%, and 17% of the HI molecules

will have one C<sub>2</sub>H<sub>2</sub> neighbor and 8% will have one HI neighbor. This implies that about 5% will have two or more acetylene neighbors.

Because of its larger size, only 59% of the C<sub>2</sub>H<sub>2</sub> molecules will be isolated, 11% will have a single HI neighbor, and 21% will have another C<sub>2</sub>H<sub>2</sub> neighbor but no HI.

There remains the question of the number of complexes, HI·C<sub>2</sub>H<sub>2</sub>, that are isolated. With 32 nearest neighbors, this turns out to be about 40%. The fraction of the complexes with another acetylene in the same cage is almost as large, 33%. The remaining 27% is distributed among a variety of multiple nearest-neighbor situations, each present in small abundance. Those complexes with other acetylenes in the same cage presumably account for the C<sub>4</sub> products.

**Vinyl Iodide** The HI·C<sub>2</sub>H<sub>2</sub> experiment offers an unequivocal identification of vinyl iodide while its growth behavior indicates that it is a primary product that undergoes secondary photolysis.

Crucial to the interpretation of our data is the question of the products of that secondary photolysis. Vinyl bromide, which has been carefully studied in matrices, provides a suitable prototype. Andrews<sup>2,3</sup> photolyzed vinyl bromide in argon and found bromoacetylene and HBr elimination as products. This same compound was photolyzed in krypton by Abrash,<sup>10</sup> and the product growth behavior was studied carefully. He also found two products, the HBr·C<sub>2</sub>H<sub>2</sub> complex and bromoacetylene, but with quite distinct growth behaviors. Whereas HBr·C<sub>2</sub>H<sub>2</sub> grew immediately, the bromoacetylene product grew with strongly sigmoidal behavior and zero slope at short photolysis times. Plainly vinyl bromide undergoes primarily photolysis to eliminate HBr, whereas HCCBr is formed only through secondary photolysis of the HBr·C<sub>2</sub>H<sub>2</sub> complex. Our evidence indicates that vinyl iodide has identical behavior, i.e., photolysis gives the elimination product HI·C<sub>2</sub>H<sub>2</sub> but not H<sub>2</sub>·HCCI.

**HCCD.** When matrices containing HI and C<sub>2</sub>D<sub>2</sub> are photolyzed, product absorptions appear that are readily associated with the spectrum of monodeuteroacetylene. By growth behavior, they can be divided into two sets, each assignable to C<sub>2</sub>HD. One set, 3334.0, 2582.1, 679.4, and 516.4 cm<sup>-1</sup>, is assigned to isolated C<sub>2</sub>HD while the other set is assigned to C<sub>2</sub>HD in the photolytically produced complex, DI·C<sub>2</sub>HD. The identification of isolated C<sub>2</sub>HD is primarily based on the growth behavior displayed in Figures 4, 7, and 9. In every case, the features at 3334.0 and 2582.1 cm<sup>-1</sup> grow initially with finite slope and grow continuously throughout photolysis. As mentioned earlier, more than half of the HI molecules will be isolated. Photolysis of these HI molecules will produce translationally hot hydrogen atoms, many of which will escape the cage. If such an H atom encounters an isolated C<sub>2</sub>D<sub>2</sub> molecule before losing its translational energy, isotopic exchange can be expected, producing a deuterium atom still with enough energy to escape the cage and leaving behind an isolated C<sub>2</sub>HD molecule.

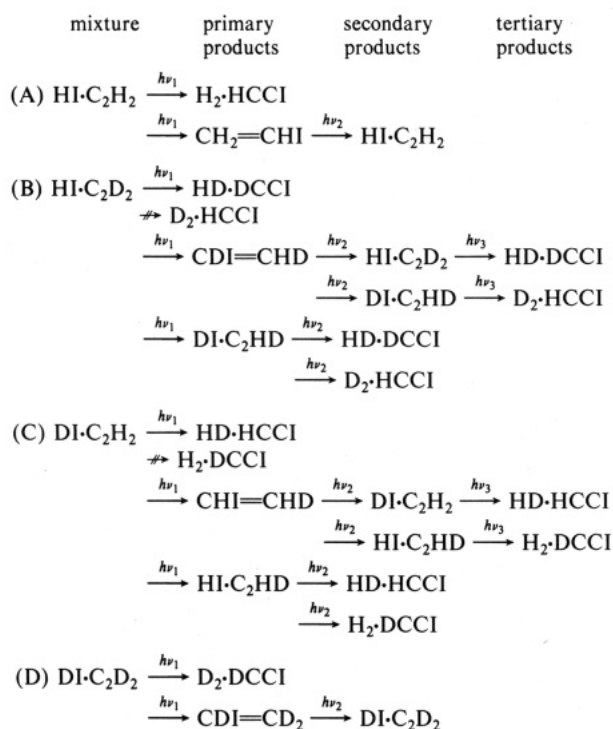


The second set of features, those attributed to DI·C<sub>2</sub>HD, grow initially with finite slope but then decrease, as typified by 3328.5 and 2577.7 cm<sup>-1</sup> in Figure 4a and Figure 4b. The decrease is plainly due to secondary photolysis, this time to form iodoacetylene, HCCI or DCCI, in the same cage with hydrogen.

**The DCCI/HCCI Ratio.** The DCCI/HCCI ratio in the HI·C<sub>2</sub>D<sub>2</sub> experiment is particularly revealing. Figure 4a shows that HCCI (3306.1 cm<sup>-1</sup>) has a growth curve with zero slope at short photolysis times. In contrast, DCCI has a finite slope at short times, even though its growth curve has a slight sigmoidal character (Figure 4b). This difference is most strikingly shown in Figure 5; at very short times the formation of HD·DCCI is at least 10 times more probable than formation of D<sub>2</sub>·HCCI. The situation is reversed in the DI·C<sub>2</sub>H<sub>2</sub> experiment (despite the minor amount of HI·C<sub>2</sub>H<sub>2</sub>). This time, Figure 8 shows that the

(10) Abrash, S. A. Ph.D. Dissertation, University of California, Berkeley, 1987.

## CHART I



DCCI/HCCI ratio is less than 0.10 for very short times. Both Figures 5 and 8 show that the hydrogen (deuterium) atom in the hydrohalide is preferentially eliminated in the molecular hydrogen product.

**Isotopic Combinations.** We now have four experimental premises with which to interpret the mixed isotope studies. When the hydrohalide-acetylene complex is photolyzed in krypton, (i) vinyl iodide is a primary product; (ii) acetylene isotopic exchange is another primary process; (iii) formation of iodoacetylene is a primary process in which the hydrohalide hydrogen exclusively ends up in the hydrogen molecule; and (iv) vinyl iodide undergoes secondary photolysis, giving only hydrohalide elimination.

The premises lead to the expectations for the mixed isotope experiments shown in Chart I. We see that in Chart I, reactions A and C, HCCI is a primary product but DCCI is not. In reactions B and D, DCCI is a primary product but HCCI is not. It is implied that in the (A) and (C) growth curves, HCCI should have a nonzero initial slope and that in (C) DCCI should have a zero initial slope, Figures 2, 7a, and 7b are in accord. The situation should reverse in (B) and (D), where DCCI should have non-zero initial slope, and in (B), HCCI should have a zero slope. Again, Figures 4a, 4b, and 9b are in qualitative agreement with expectations. (Of course, (C) and (D) are complicated somewhat by the minor presence of HI in our samples.) Thus, the recorded growth behaviors are all consistent with the four premises listed earlier and the mechanisms presented in (A), (B), (C), and (D). Premises iii and iv are perhaps the most interesting and least predictable on the basis of simple thermochemical arguments.

## Thermochemistry

Figure 10 shows the energy relationships that exist among reactants and products.<sup>11</sup> The energies for [HI]\* are vertical transition energies for gaseous HI, thus ignoring any excited-state interaction with the neighboring C<sub>2</sub>H<sub>2</sub>.<sup>12</sup> Evidently there is

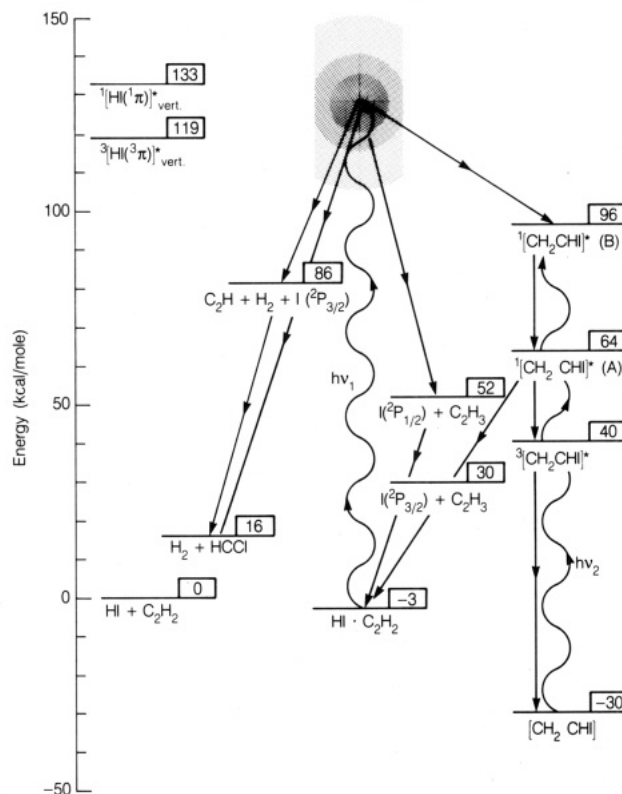


Figure 10. Energy diagram for the photolysis of HI-C<sub>2</sub>H<sub>2</sub> complexes in Kr.

enough energy to produce vinyl iodide in either its first excited singlet or triplet state. After internal conversion, either state would have ample energy to eliminate H<sub>2</sub> to produce HCCI but our premise iv indicates that this channel is a minor one. Most of the excited vinyl iodide returns to the parent complex (effecting isotopic exchange) or relaxes to ground-state vinyl iodide.

We see that photoproduction of vinyl iodide and its secondary photolysis only catalyze isotopic exchange. We deduce that the mechanism by which iodoacetylene is formed does not involve vinyl iodide or its excited state.

To picture a mechanism by which iodoacetylene is formed as a primary product, we observe, first, that the hydrohalide excitation tends to impart high translational energy to its hydrogen (deuterium) atom. Then we note that our results show that the "ejected" hydrogen (deuterium) atom ends up in product hydrogen molecules. This suggests that the process by which iodoacetylene is formed can be pictured as an abstraction, as in the following sequence of reactions, all within the cage:



We speculate that the geometry of the initial complex accounts for the high selectivity in this abstraction process.

## Conclusion

The photolysis of hydrogen iodide-acetylene hydrogen-bonded complexes in solid krypton produces both iodoacetylene and vinyl iodide in primary processes. Secondary photolysis of vinyl iodide quickly catalyzes isotopic exchange in isotopic mixtures, but it does not directly produce iodoacetylene. We conclude that the primary production of iodoacetylene involves hydrogen (deuterium) atom abstraction from acetylene by the energetic hydrogen iodide.

(11) Excited states of HI, ref 12;  $\Delta H^\circ_f$ 's (kcal/mol) C<sub>2</sub>H<sub>3</sub>, 59.6 or 71.8, ref 13a,b; C<sub>2</sub>H, 135, ref 14; HCCI, 77, ref 15; CH<sub>2</sub>CHI, 30.8, ref 16; excited states of vinyl iodide, ref 17.

(12) Chapman, D. A.; Balasubramanian, Lin, S. H. *Chem. Phys. Lett.* **1985**, *118*, 192.

(13) (a) 59.6 kcal/mol; Lossing, F. P. *Can. J. Chem.* **1971**, *49*, 357. (b) 71.8 kcal/mol; DeFrees, D. J.; McIver, Jr., R. T.; Hehre, W. J. *J. Am. Chem. Soc.* **1980**, *102*, 3334.

(14) Calculated using  $D_0(\text{C}_2\text{H-H}) = 132 \pm 2$  kcal/mol from: Wodtke, A. M. and Lee, Y.-T. *J. Phys. Chem.* **1985**, *89*, 4744. (Note: this  $\Delta H^\circ_f$  may be too high by about 15 kcal/mol.)

(15) Okabe, H. *J. Chem. Phys.* **1975**, *62*, 2782.

(16) Benson, S. W. *Thermochemical Kinetics*; Wiley: New York, 1976; p 297.

(17) A and B states: Boschi, R. A.; Salahub, D. R. *Mol. Phys.* **1972**, *24*, 735; triplet state from C<sub>2</sub>H<sub>4</sub>, see: Lee, Y. P.; Pimentel, G. C. *J. Chem. Phys.* **1981**, *75*, 4241.

We shall be seeking additional evidence about this mechanism by investigating the branching yield as a function of photolysis wavelength.<sup>4</sup>

*Acknowledgment.* This work was supported by the Director, Office of Energy Research, Office of Basic Energy Sciences,

Chemical Sciences Division, of the U.S. Department of Energy under Contract No. DE-AC03-76SF00098.

**Registry No.** HI, 10034-85-2; C<sub>2</sub>H<sub>2</sub>, 74-86-2; CH<sub>3</sub>CHI, 593-66-8; HCCI, 14545-08-5; C<sub>2</sub>D<sub>2</sub>, 1070-74-2; DI, 14104-45-1; DCCI, 14545-09-6.

## Wavelength Dependence of the Photochemistry of Hydrogen Iodide-Acetylene Complexes in Solid Krypton

Samuel A. Abrash<sup>†</sup> and George C. Pimentel<sup>\*‡</sup>

Laboratory of Chemical Biodynamics, Lawrence Berkeley Laboratory, University of California, Berkeley, California 94720 (Received: January 27, 1989)

Hydrogen iodide-acetylene complexes in a krypton matrix at 12 K have been photolyzed at fixed wavelengths in the range 222-308 nm. Products are identified with infrared spectroscopy. With deuterium substitutions (HI-C<sub>2</sub>D<sub>2</sub> and DI/HI/C<sub>2</sub>H<sub>2</sub>), three product channels are identified leading to isotopic exchange, formation of vinyl iodide, and formation of iodoacetylene. At wavelengths longer than 300 nm, only iodoacetylene is formed whereas at shorter wavelengths, isotopic exchange occurs (e.g., HI-C<sub>2</sub>D<sub>2</sub> → DI-C<sub>2</sub>HD), vinyl iodide is formed, and some iodoacetylene is formed. Because the T-shaped geometry of the HI-C<sub>2</sub>H<sub>2</sub> complex is well established, it is possible to interpret these results by recognizing that the photolysis involves two molecules in proximity, a *supramolecule*. As the hydrogen atom leaves the iodine atom, it forms initially C<sub>2</sub>H<sub>3</sub>. Correlating the energy levels along this initial reaction coordinate indicates the initial photolytic reaction surfaces, and Franck-Condon arguments explain the wavelength dependence of the product distribution. This supramolecule analysis provides a prototype analysis for other examples of photolysis of bound and geometrically constrained complexes.

### Introduction

Photolysis of hydrogen iodide-acetylene complexes in solid krypton results in two products, iodoacetylene and vinyl iodide, as well as exchange in isotopic mixtures.<sup>1</sup> This outcome raises the question of the extent to which the excitation behavior is a function of the six-atom entity defined by the HI-C<sub>2</sub>H<sub>2</sub> complex. Even though the complex is sufficiently weakly bound that the ground state can be regarded as two weakly interacting molecular components, it is quite unlikely that this situation persists for the excited species. Instead, the upper electronic states and their chemistries are more likely to be properties of the six-atom system, which we will call the *supramolecule*.

To test this point of view, we have investigated the effect of excitation wavelength on the branching for this hydrogen iodide-acetylene system. Tuned laser photolysis has been used over the wavelength range 222-309 nm; most attention has been focused on isotopic combinations that help identify primary and secondary photolytic processes.

### Experimental Section

The cryostat, spectrometer, mixture preparation, chemicals, and deposition conditions were identical with those described in paper 1.<sup>1</sup> Photolysis conditions differed as described below.

The laser was a Quanta Ray YAG pumped dye laser. The pump laser was a DCR-2A optimized for a repetition rate of 10 Hz. The 1064-nm beam from the DCR was directed into a harmonic generator (Quanta Ray Model HG-2), where the 532-nm green beam was generated, and through the Quanta Ray prism harmonic separator (PHS-1), where the green beam and the fundamental were spatially separated. The green beam and, in some applications, the 1064-nm beam were then directed through different ports into the dye laser (Quanta Ray, Model PDL). The green beam was then used to pump the dye beam which was directed into the Quanta Ray wavelength extender

TABLE I: Spectral Features of Hydrogen Iodide-Acetylene Photolysis Products in Solid Krypton<sup>1</sup>

	$\nu$ , cm <sup>-1</sup>		$\nu$ , cm <sup>-1</sup>	
CH <sub>2</sub> CHI	1587.2	HCCD	3328.5	
	1386.2		2577.7	
	1237.3		516.4	
HCCI	952.1	DCCI	2584.0	
	3305.8		1975.2	
	2053.5			
HCCCCI	625.7/624.1/623.8	HI (isolated)	2231.5	
	3314.6		DI (isolated)	1599.5
	1234.9			
I-H...C≡C	625			
I-H...C≡C	2179.4			
I-D...C≡C	1562.4			

(WEX). The WEX was used to double the dye beam and, in some cases, to sum the resulting UV photons with the 1064-nm YAG fundamental. The final beam was then directed through four UV quartz right-angle prisms (Optics for Research and Oriel) to the sample. Quanta Ray specifications for pulse width and pulse to pulse energy variance were 10 ns and 5%, respectively. The specification for the line width was 0.25 cm<sup>-1</sup>.

All laser dyes were obtained from Exciton; they included Rhodamine 590, Sulforhodamine 640, DCM, and LDS 698. Methanol was used as solvent (Mallinckrodt, Spectro Grade or Semiconductor Grade). These dyes provided a wavelength range of 276.2-356.7 nm for the dye second harmonic and from 222.4 to 267.1 nm for the second harmonic + 1064 nm. The wavelength dial on the dye laser was calibrated by using a monochromator (McKee Pederson Instruments, Model MP1018) which was, in turn, calibrated to ±0.1 nm by using the second harmonic of the YAG (532.0) and the red beam of a He-Ne laser (632.9 nm).

Average power was measured with a power meter (Sciencetech, Model 380105) optimized for operation between 200 and 400 nm, whose output was read from a digital multimeter (Keithly, Model

<sup>†</sup> Present address: Department of Chemistry, University of Pennsylvania, Philadelphia, PA 19123.

<sup>‡</sup> Deceased June 18, 1989.

(1) Abrash, S. A.; Pimentel, G. C. *J. Phys. Chem.*, preceding paper in this issue. Hereafter, this paper will be called paper 1.